

# Structures of Substituted-Cyclopentadienyl Uranium(III) Dimers and Related Uranium Metallocenes Deduced by EXAFS

Wayne W. Lukens, Jr., Patrick G. Allen, Jerome J. Bucher,  
Norman M. Edelstein, Eric A. Hudson, David K. Shuh, Tobias Reich,<sup>†</sup> and  
Richard A. Andersen\*

Chemistry Department and Chemical Sciences Division of Lawrence Berkeley Laboratory,  
University of California, Berkeley, California 94720

Received July 14, 1998

The crystal structures of  $[\text{Cp}''_2\text{UF}]_2$  and  $[\text{Cp}^+_2\text{UO}]_2$  are reported, where  $\text{Cp}''$  is 1,3-( $\text{Me}_3\text{-Si}$ ) $_2\text{C}_5\text{H}_3$  and  $\text{Cp}^+$  is 1,3-( $\text{Me}_3\text{C}$ ) $_2\text{C}_5\text{H}_3$ . Both complexes have idealized  $C_{2h}$  symmetry, and their  $\text{U}\cdots\text{U}$  distances are 3.85 and 3.39 Å, respectively. The X-ray absorption spectra of several uranium metallocene complexes, and the numerical results from fitting the EXAFS spectra, are reported. For  $[\text{Cp}^+_2\text{UF}]_2$ , the  $\text{U}\cdots\text{U}$  distance was found by EXAFS to be similar to that in  $[\text{Cp}''_2\text{UF}]_2$ , implying that  $[\text{Cp}^+_2\text{UF}]_2$  is dimeric. A structural model is advanced that correlates the  $\text{U}\cdots\text{U}$  distance with the orientation of the cyclopentadienyl rings; the orientation is due to a subtle combination of steric repulsions between ligands on the same metal center and between ligands on adjacent metal centers.

## Introduction

During a variable-temperature  $^1\text{H}$  NMR spectroscopic study of the solution dynamics of the uranium(III) dimers  $[\text{Cp}''_2\text{UX}]_2$  and  $[\text{Cp}^+_2\text{UX}]_2$ , where  $\text{Cp}''$  is 1,3-( $\text{Me}_3\text{-Si}$ ) $_2\text{C}_5\text{H}_3$ ,  $\text{Cp}^+$  is 1,3-( $\text{Me}_3\text{C}$ ) $_2\text{C}_5\text{H}_3$ , and X is a halide, the behavior of the fluorides  $[\text{Cp}''_2\text{UF}]_2$  and  $[\text{Cp}^+_2\text{UF}]_2$  was found to be substantially different from that of the other halide dimers.<sup>1,2</sup> The low-temperature solution  $^1\text{H}$  NMR chemical shifts of the heavier halide dimers were satisfactorily interpreted on the basis of the observed solid-state structures of these complexes. As a first step toward understanding the solution dynamics of the fluoride complexes, single-crystal X-ray structure analysis was required for each. Unfortunately, while  $[\text{Cp}''_2\text{-UF}]_2$  crystallizes well, suitable crystals of  $[\text{Cp}^+_2\text{UF}]_2$  could not be obtained. The lack of a crystal structure of  $[\text{Cp}^+_2\text{UF}]_2$  led to our use of EXAFS spectroscopy to assist in the structural characterization of organouranium complexes, since this technique will give the  $\text{U}\cdots\text{U}$  distances and, therefore, the nature of the aggregation of the complexes in the solid state.

The low-temperature NMR spectrum of  $[\text{Cp}^+_2\text{UF}]_2$  shows six inequivalent  $\text{CMe}_3$  groups. As described earlier, this observation can be rationalized in one of three ways. The complex could be a trimer with  $C_2$  symmetry, as is  $[(\text{Me}_5\text{C}_5)_2\text{UCl}]_3$ ,<sup>3</sup> the molecule could

exist as a mixture of conformers, one with  $D_2$  or  $C_{2h}$  symmetry having two inequivalent  $\text{CMe}_3$  groups and one with  $C_2$ ,  $C_s$ , or  $C_i$  symmetry having four inequivalent  $\text{CMe}_3$  groups, or the molecule could exist as a single conformer with  $C_{2h}$  symmetry in which the  $\text{CMe}_3$  groups do not rotate. The EXAFS spectrum of  $\text{Cp}^+_2\text{UF}$  shows that the molecule is not a cyclic trimer. In a cyclic trimer, the  $\text{U-F-U}$  unit will be nearly linear, as in  $[(\text{Me}_5\text{C}_5)_2\text{UCl}]_3$ ,<sup>3</sup> therefore, the  $\text{U}\cdots\text{U}$  distance will be substantially longer than the  $\text{U}\cdots\text{U}$  distance in a dimer with two bridging fluoride ligands where the  $\text{U-F-U}$  angles are considerably less than linear. When the  $\text{U}\cdots\text{U}$  distance in  $[\text{Cp}^+_2\text{UF}]_2$  is compared to those in other complexes, the nuclearity of the complex can be determined with certainty. In this paper, we develop the use of EXAFS in this structural problem by comparing the EXAFS data with known metrical parameters derived from single-crystal X-ray results, when known. In this way, the confidence in the application of the EXAFS deductions to molecules whose single-crystal structure is unknown is increased.

## Results

The solid-state structure of  $[\text{Cp}''_2\text{UF}]_2$  is shown in Figure 1, and selected distances and angles are given in Table 1. Two crystallographically independent but virtually identical molecules are found in the unit cell. The structure of the complex is similar to that of  $[\text{Cp}''_2\text{-UCl}]_2$ .<sup>1</sup> The major difference between the chloride and fluoride structures is that the  $\text{U}\cdots\text{U}$  distance in the fluoride is more than 1 Å shorter than in  $[\text{Cp}''_2\text{UCl}]_2$ ! One consequence of the shorter  $\text{U}\cdots\text{U}$  distance is the slightly different orientation of the  $\text{Cp}''$  ligands in the complexes. While the symmetry of  $[\text{Cp}''_2\text{UCl}]_2$  is  $C_i$ , the idealized symmetry of  $[\text{Cp}''_2\text{UF}]_2$  is  $C_{2h}$  (the crystallographic symmetry is also  $C_i$ ). In addition, the  $\text{F-U-F}$

\* To whom correspondence should be addressed at the Chemistry Department, University of California.

<sup>†</sup> Present address: Institut für Radiochemie, Forschungszentrum, Rossendorf, Postfach 510119, D-0134 Dresden, Germany.

(1) (a) Blake, P. C.; Lappert, M. F.; Taylor, R. G.; Atwood, J. L.; Hunter, W. E.; Zhang, H. *J. Chem. Soc., Chem. Commun.* **1986**, 1394–1395. (b) Blake, P. C.; Lappert, M. F.; Taylor, R. G.; Atwood, J. L.; Zhang, H. *Inorg. Chim. Acta* **1987**, *129*, 12.

(2) Lukens, W. W., Jr.; Beshouri, S. M.; Stuart, A. L.; Andersen, R. A. *Organometallics* **1999**, *18*, 1247–1252.

(3) Fagan, P. J.; Manriquez, J. M.; Marks, T. J.; Day, C. S.; Vollmer, S. H.; Day, V. W. *Organometallics* **1982**, *1*, 170–180.

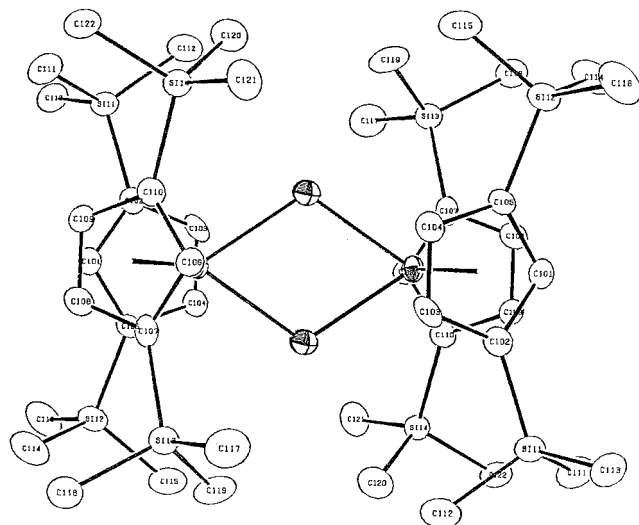


**Figure 1.** ORTEP drawing of one of two crystallographically independent molecules of  $[\text{Cp}''_2\text{UF}]_2$ .

**Table 1.** Selected Distances (Å) and Angles (deg) in  $[\text{Cp}''_2\text{UF}]_2^{a,b}$

molecule 1		molecule 2	
U1–U1'	3.844(1)	U2–U2'	3.851(1)
U1–F1	2.331(3)	U2–F2	2.334(3)
U1–F1'	2.332(3)	U2–F2'	2.333(3)
U1–Cp11	2.49	U2–Cp21	2.49
U1–Cp12	2.49	U2–Cp22	2.49
U1–(Cring)	2.766(8)	U2–(Cring)	2.768(9)
F1–U1–F1'	68.9(1)	F2–U2–F2'	68.8(1)
U1–F1–U1'	111.1(1)	U2–F2–U2'	111.2(1)
Cp11–U1–Cp12	130.4	Cp21–U2–Cp22	129.7

<sup>a</sup> The atoms with a prime symbol are related by inversion symmetry to the atoms without a prime symbol. <sup>b</sup> Cp11, Cp12, Cp21, and Cp22 are the centroids of the cyclopentadienyl rings.

angle is only 69°, much more acute than the Cl–U–Cl angle of 78°. The U–F distance is 0.48 Å shorter than the U–Cl distance of 2.818(4) Å, in agreement with the difference in radii of fluoride and chloride ions.<sup>4</sup> Steric congestion resulting from the short U···U distance forces the SiMe<sub>3</sub> groups to bend by an average of 9° out of the plane defined by the Cp'' ring carbon atoms. Since the radius of O<sup>2-</sup> (1.40 Å)<sup>4</sup> is similar to that of F<sup>-</sup> (1.36 Å),<sup>4</sup> the X-ray structure of a metallocene U(IV) dimer with bridging oxide ligands should strengthen these deductions about intramolecular ring···ring repulsions, ring conformations, and metal···metal distances.

The solid-state structure of  $[\text{Cp}^{\ddagger}_2\text{UO}]_2$  is shown in Figure 2, and selected distances and angles are given in Table 2. One of the CMe<sub>3</sub> groups is disordered, but, for clarity, only one set of disordered Me positions is shown in Figure 2. The structure of  $[\text{Cp}^{\ddagger}_2\text{UO}]_2$  is almost identical with that of  $[\text{Cp}''_2\text{UO}]_2$ .<sup>5</sup> The U···U distance in both complexes is very short at 3.39 Å, and both dimeric oxometallocenes have the same idealized  $C_{2h}$  structure as  $[\text{Cp}''_2\text{UF}]_2$ . As in  $[\text{Cp}''_2\text{UF}]_2$ , the quaternary carbon atoms are bent out of the plane of the Cp ring by 11°. The orientations of the Cp<sup>‡</sup> rings in the metal-

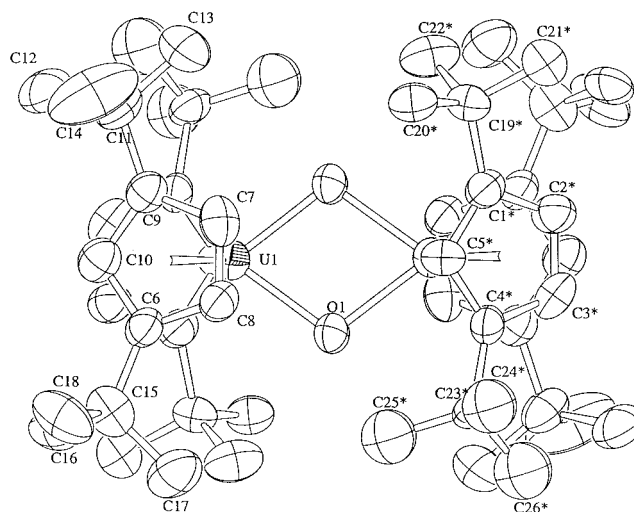


**Figure 2.** ORTEP drawing of  $[\text{Cp}^{\ddagger}_2\text{UO}]_2$ .

**Table 2.** Distances (Å) and Angles (deg) in  $[\text{Cp}^{\ddagger}_2\text{UO}]_2$  and  $[\text{Cp}''_2\text{UO}]_2^{a,b}$

$[\text{Cp}^{\ddagger}_2\text{UO}]_2$		$[\text{Cp}''_2\text{UO}]_2^5$	
U–U'	3.390(1)	U–U'	3.393(1)
U–O	2.118(7)	U–O	2.096(6)
U–O'	2.121(7)	U–O'	2.129(5)
U–Cp1	2.53	U–Cp1	2.50
U–Cp2	2.52	U–Cp2	2.49
U–(Cring)	2.80(4)	U–(Cring)	2.7(2)
Cp1–U–Cp2	124	Cp1–U–Cp2	123
O–U–O'	73.8(3)	O–U–O'	73.2(2)
U–O–U'	106.2(3)	U–O–U'	106.8(2)

<sup>a</sup> The atoms with a prime symbol are related by inversion symmetry to the atoms without a prime symbol. <sup>b</sup> Cp1 and Cp2 are the centroids of the cyclopentadienyl rings.

locene U(III) and U(IV) dimers are dictated by intramolecular steric interactions, especially the U···U distance.<sup>2</sup>

The X-ray absorption spectra of several organouranium(III) and -(IV) complexes were obtained, and numerical results of fitting the EXAFS spectra are given in Table 3 along with bond distances determined by crystallography, when these data are known. These comparisons are important, since they determine the validity with which the EXAFS results can be used for the resolution of structural problems in actinide chemistry and in organoactinide chemistry in particular. Plots of the spectra, fits, and their Fourier transforms are shown in Figure 3. The theoretical phases and amplitudes for fitting the spectra were calculated using the program Feff<sup>6</sup> with atomic coordinates from the crystal structures.<sup>1,5,7</sup> Where the crystal structure of the complex was not known, the U–X and U···U distances were changed according to the radius of X or to the distance in a close analogue whose crystal structure was known.

One problem encountered in the analysis of almost all of the EXAFS spectra was a correlation between the Debye–Waller factors of the Cp carbon atoms and those of the halide atoms. Either one of the Debye–Waller factors would become small and the other quite large or both of them would become quite small. This problem

(4) Pauling, L. *The Nature of the Chemical Bond*; Cornell University Press: Ithaca, NY, 1960.

(5) Zalkin, A.; Beshouri, S. *Acta Crystallogr.* **1988**, *C44*, 1826–1827.

(6) Rehr, J. J.; Zabinsky, S. I.; Albers, R. D. *Phys. Rev. Lett.* **1992**, *69*, 3397.

(7) Zalkin, A.; Stuart, A. L.; Andersen, R. A. *Acta Crystallogr.* **1988**, *C44*, 2106–2108.

**Table 3. EXAFS Data for Organouranium Complexes and Comparison between Single-Crystal X-ray Crystallographic Data**

scattering atom	no. of atoms	$\sigma^2$ (Å <sup>2</sup> ) <sup>a</sup>	distance (Å) <sup>b</sup>	
			EXAFS	crystallography
[Cp <sup>''</sup> <sub>2</sub> UF] <sub>2</sub>				
F	2	0.0064	2.318(6)	2.331(3)
C <sub>ring</sub>	10	0.0140*	2.78(1)	2.767(8)
U	1	0.0074	3.89(1)	3.845(1)
[Cp <sup>''</sup> <sub>2</sub> UCl] <sub>2</sub>				
C <sub>ring</sub>	10	0.0120*	2.731(6)	2.78(2)
Cl	2	0.0047	2.806(3)	3.81(1)
U	1	0.0056	4.306(9)	4.357(1)
[Cp <sup>+</sup> <sub>2</sub> UF] <sub>2</sub>				
F	2	0.0048	2.285(6)	
C <sub>ring</sub>	10	0.0153	2.82(1)	
U	1	0.0045	3.840(8)	
[Cp <sup>+</sup> <sub>2</sub> UCl] <sub>2</sub>				
C <sub>ring</sub>	10	0.0120*	2.76(1)	2.78(4)
Cl	2	0.0064	2.859(6)	2.856
U	1	0.0060	4.55(2)	4.540(1)
[Cp <sup>+</sup> <sub>2</sub> UBr] <sub>2</sub>				
C <sub>ring</sub>	10	0.0120*	2.757(7)	
Br	2	0.0104	2.973(5)	
U	1	0.0079	4.62(2)	
[Cp <sup>+</sup> <sub>2</sub> UO] <sub>2</sub>				
O	2	0.0184	2.21(1)	2.121(7)
C <sub>ring</sub>	10	0.0120*	2.821(6)	2.80(4)
U	1	0.0028	3.395(3)	3.390(1)
Cp <sup>''</sup> <sub>2</sub> UBr <sub>2</sub>				
C <sub>ring</sub>	10	0.0121	2.704(8)	2.71(1)
Br	2	0.0046	2.744(3)	2.734(1)
Cp <sup>+</sup> <sub>2</sub> UBr <sub>2</sub>				
C <sub>ring</sub>	10	0.0120*	2.702(8)	
Br	2	0.0050	2.742(3)	
Cp <sup>+</sup> <sub>2</sub> UI <sub>2</sub>				
C <sub>ring</sub>	10	0.0104	2.724(3)	
I	2	0.0052	2.974(1)	

<sup>a</sup>  $\sigma^2$  values are Debye–Waller factors; fixed factors are indicated by asterisks. <sup>b</sup> The number in parentheses is the standard deviation.

was treated by fixing the Debye–Waller factor of the Cp carbon atoms to 0.012. This value was chosen because this parameter could be refined in a few cases, [Cp<sup>+</sup><sub>2</sub>UF]<sub>2</sub>, [Cp<sup>+</sup><sub>2</sub>UBr]<sub>2</sub>, Cp<sup>+</sup><sub>2</sub>UBr<sub>2</sub>, Cp<sup>+</sup><sub>2</sub>UI<sub>2</sub>, and Cp<sup>''</sup><sub>2</sub>UBr<sub>2</sub>, and was found to vary from 0.010 to 0.015. In addition, the use of this value resulted in good agreement of the U–C distances with those obtained by crystallography.

In some cases, the Fourier transforms of the EXAFS appear to have additional features at  $R \approx 3.7$ , possibly due to scattering from the silicon of the Cp<sup>''</sup> ligand or from the tertiary carbon of the Cp<sup>+</sup> ligand. These features are most apparent in parts a and c of Figure 3. Attempts to fit these features produced unreasonably small ( $\sigma^2 \approx 0.001$ ) Debye–Waller factors in the case of the scattering from the tertiary carbon. Although inclusion of this shell improved the quality of the fit, it did not appreciably change the values of the other parameters. Since the Debye–Waller factors seemed unreasonable and addition of this shell had little effect upon the other parameters, it was not included.

### Discussion

While the overall agreement between bond distances determined by EXAFS and crystallography is good,

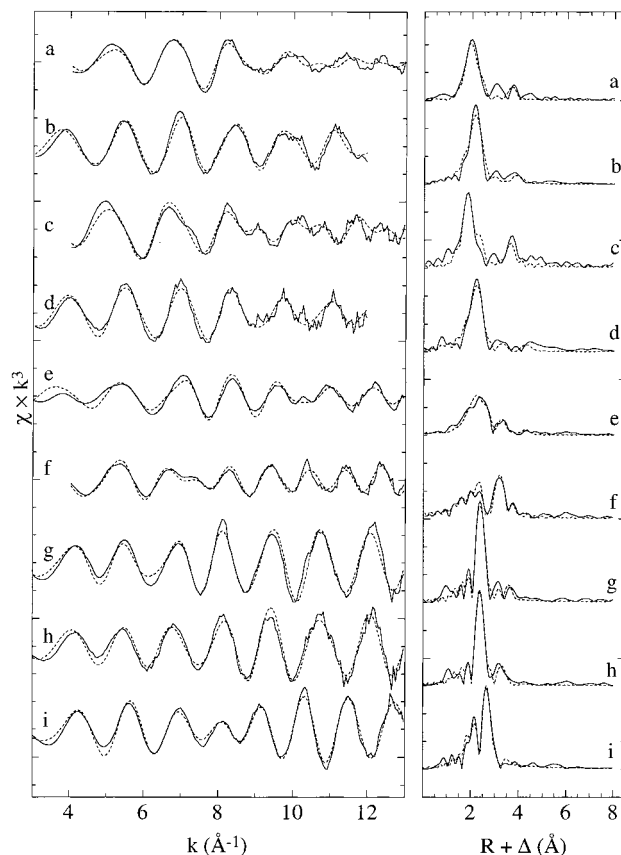


**Figure 3.** EXAFS (left side) spectra (dotted lines) and fits (solid lines) and Fourier transforms (right side) for (a) [Cp<sup>''</sup><sub>2</sub>UF]<sub>2</sub>, (b) [Cp<sup>''</sup><sub>2</sub>UCl]<sub>2</sub>, (c) [Cp<sup>+</sup><sub>2</sub>UF]<sub>2</sub>, (d) [Cp<sup>+</sup><sub>2</sub>UCl]<sub>2</sub>, (e) [Cp<sup>+</sup><sub>2</sub>UBr]<sub>2</sub>, (f) [Cp<sup>+</sup><sub>2</sub>UO]<sub>2</sub>, (g) Cp<sup>''</sup><sub>2</sub>UBr<sub>2</sub>, (h) Cp<sup>+</sup><sub>2</sub>UBr<sub>2</sub>, and (i) Cp<sup>+</sup><sub>2</sub>UI<sub>2</sub>.

some of the differences are large. For [Cp<sup>''</sup><sub>2</sub>UF]<sub>2</sub>, the U···U distances determined from EXAFS and X-ray crystallography differ by 0.05 Å; this error, 1% of the distance, is typical for EXAFS.<sup>9b</sup> Differences which are greater than 1% of the bond length are present in the U–C<sub>ring</sub> distance of [Cp<sup>''</sup><sub>2</sub>UCl]<sub>2</sub> and the U–O distance of [Cp<sup>+</sup><sub>2</sub>UO]<sub>2</sub>; this error is believed to arise from the previously mentioned problem of correlation between the fitted parameters of the two inner shells.

Apart from these exceptions, the EXAFS data for these organouranium complexes show a close correspondence to the crystal structure data when the latter data are available, and when the single-crystal X-ray structure is not known, the data agree with those for similar structures. For [Cp<sup>+</sup><sub>2</sub>UBr]<sub>2</sub>, which presumably has the same structure as [Cp<sup>+</sup><sub>2</sub>UCl]<sub>2</sub>, the U–Cp and U–U distances are identical to within 3 $\sigma$ , and the U–Br distance is close to that found in [Cp<sup>''</sup><sub>2</sub>UBr]<sub>2</sub>, 2.94(1) Å.<sup>1a</sup> For Cp<sup>+</sup><sub>2</sub>UBr<sub>2</sub> and Cp<sup>+</sup><sub>2</sub>UI<sub>2</sub>, the uranium–halide distances are similar to those found in Cp<sup>''</sup><sub>2</sub>UBr<sub>2</sub> and Cp<sup>''</sup><sub>2</sub>UI<sub>2</sub>, 2.734(1) and 2.953(2) Å, respectively.<sup>1b</sup>

For [Cp<sup>+</sup><sub>2</sub>UF]<sub>2</sub>, the U···U distances and U–F distances are almost identical with those in [Cp<sup>''</sup><sub>2</sub>UF]<sub>2</sub>. In addition, the U–Cp(centroid) distance in [Cp<sup>+</sup><sub>2</sub>UF]<sub>2</sub> is long,

(8) DeKock, R. L.; Peterson, M. A.; Reynolds, L. E. L.; Chen, L.-H.; Baerends, E. J.; Vernooijs, P. *Organometallics* **1993**, *12*, 2794–2805.

(9) (a) *X-ray Absorption, Principles, Applications, Techniques of EXAFS, SEXAFS, and XANES*; Koningsberger, D. C., Prins, R., Eds.; Wiley: New York, 1988. (b) Teo, B. K. *EXAFS: Basic Principles and Data Analysis*; Springer-Verlag: Berlin, 1986.

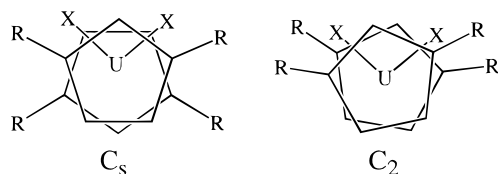


**Figure 4.**  $Cp''$  and  $Cp^+$  ligand conformations observed among dicyclopentadienyluranium halide dimers (only one metallocene fragment of the dimer is shown).

almost equal to that of  $[Cp^+_2UO]_2$ . The long U–Cp (centroid) distance in  $[Cp^+_2UO]_2$  is presumably due to repulsions between  $CMe_3$  groups of different  $Cp^+$  ligands on the same metal center. The similarity between these structural parameters is consistent with the postulate that  $[Cp^+_2UF]_2$  has the same  $C_{2h}$  structure as the oxo dimer. Although the symmetry of  $[Cp^+_2UF]_2$  is impossible to determine with certainty from these data, it is definitely dimeric. The short U...U distance is inconsistent with a trimeric formulation, since the U...U distance in a hypothetical trimer would be approximately 4.5 Å, nearly twice the length of a U–F bond. The observed U...U distance of 3.84 Å is, therefore, inconsistent with a trimeric formulation for this complex.

While the molecular structure of  $[Cp''_2UF]_2$  is similar to that of  $[Cp''_2UCl]_2$ , the structure of  $[Cp^+_2UO]_2$  is considerably different from that of  $[Cp^+_2UCl]_2$ . Among these complexes, only two ring conformations are observed,  $C_s$  and  $C_2$ , as shown in Figure 4. The  $C_2$  conformation seems to be preferred for the dimeric  $Cp^+$  complexes, while the  $C_s$  conformation is preferred for the  $Cp''$  complexes. The preferred conformation is determined by the competition between steric interactions between the Cp ligands on one metal center and steric interactions between Cp ligands on adjacent metal centers. If the steric interactions between ligands on a single metal center dominate, the  $Cp_2U$  fragment adopts the  $C_2$  conformation, but if steric interactions between ligands on adjacent metal centers dominate, the  $Cp_2U$  fragment adopts a  $C_s$  conformation. In complexes with short U...U distances, such as  $[Cp^+_2UO]_2$ , the steric interactions between ligands on adjacent metal centers dominate. As a result, all of the  $Cp^+_2U$  metallocenes with U...U distances of less than ca. 3.9 Å have the  $C_s$  conformation for the  $Cp_2U$  fragment and idealized  $C_{2h}$  symmetry for the dimeric molecule as a whole.

When the U...U distance is longer, the steric interactions between ligands on adjacent metal centers are smaller. Because the Si–C bond is longer than the C–C bond, steric interactions of  $Cp''$  ligands on adjacent metallocene centers still dominate, and the  $Cp''_2U$  groups adopt the  $C_s$  structure. However, the symmetry of the dimeric molecules is lower due to the  $Cp''$  ligand orientation, presumably adopted to reduce the steric interactions between  $Cp''$  ligands on the same metal center. For the  $Cp^+_2U$  fragment, the steric interactions between ligands on the same metal center are greater than those for the  $Cp''_2U$  fragment, and steric interactions between ligands on adjacent metal centers are smaller. This difference can be illustrated by comparing the closest intramolecular contacts in  $[Cp''_2UO]_2$  and  $[Cp^+_2UO]_2$ , which have the same  $C_{2h}$  symmetric structure. The two closest contacts between Cp ligands on the same metal center is shorter (3.65 Å) in  $[Cp^+_2UO]_2$ ,

relative to 3.83 Å in  $[Cp''_2UO]_2$ .<sup>7</sup> Furthermore, in both cases, the contact is between a Cp ring carbon atom and a methyl carbon atom rather than between two methyl carbon atoms. Conversely, the closest contact between ligands on adjacent metal centers is shorter (3.91 Å) in  $[Cp''_2UO]_2$  relative to 4.16 Å in  $[Cp^+_2UO]_2$  and this contact distance is between methyl carbon atoms. As the U...U distance increases, the  $Cp^+$  ligands rearrange to minimize the steric interaction between  $Cp^+$  ligands on the same metal center, which can be accomplished by adopting the  $C_2$  conformation. In  $[Cp^+_2UCl]_2$ , the closest contact between  $Cp^+$  ligands on the same metal center is 3.76 Å and is between methyl carbon atoms. This geometry is at the expense of increasing the steric interaction between  $Cp^+$  ligands on adjacent metal centers, since their closest contact is 3.88 Å. The increased steric interaction results in an increased U...U distance in  $[Cp^+_2UCl]_2$ , some 0.18 Å longer than in  $[Cp''_2UCl]_2$ , in which the  $Cp''_2U$  fragments adopt the  $C_s$  geometry. DeKock has discussed the somewhat related metallocene dimers of the type  $Cp_4Zr_2(\mu-X)_2$ , and his results, which are based upon force field calculations relative to the solid-state crystal structures, are similar to those reached here; viz., metal...metal distances are correlated with intra- and inter-metallocene ring conformations.<sup>8</sup>

## Conclusion

The crystal structures of two dimers,  $[Cp''_2UF]_2$  and  $[Cp^+_2UO]_2$ , have been determined. Both complexes have  $C_{2h}$  symmetric structures in the solid state. EXAFS spectra of several organouranium complexes have been measured and interpreted. The distances determined using EXAFS are in good agreement with the distances determined by crystallography. For  $[Cp^+_2UF]_2$ , where the solid-state structure was unknown, the EXAFS data suggest that this molecule is dimeric and that it most likely has  $C_{2h}$  symmetry. The origin of the conformations of the  $Cp''$  and  $Cp^+$  ligands in these dimers is ascribed to a subtle combination of the steric interactions between ligands on the same metal center and between ligands on adjacent metal centers.

## Experimental Section

The compounds were prepared as previously reported.<sup>1,2</sup> EXAFS samples were prepared in an inert-atmosphere box as follows. A  $5 \times 20$  mm hole was cut into a  $3 \times 3$  cm piece of  $5 \times 10^{-3}$  inch thick Mylar film, and one side of the hole was sealed with Mylar tape. The powdered sample was evenly distributed in the hole and held in place with Mylar tape. The entire sample was then successively sealed inside of three  $3 \times 10^{-3}$  inch thick Mylar bags using an impulse sealer. The bagged samples were then placed in glass jars, which were capped and sealed with PTFE tape inside the glovebox. The jars were removed from the drybox and opened just before the samples were mounted at the beam line. Some decomposition of the samples had occurred after 5 h of exposure to air, as judged by their L3 edge shifts to higher energy and by the darkening of the samples.

The X-ray absorption spectra were acquired at SSRL at beamlines 4-1 and 4-3 using a Si(220) double-crystal monochromator detuned 50% to reduce the higher order harmonic content of the beam. The data were obtained in the transmission mode at room temperature using argon-filled ionization

chambers and referenced to the first inflection point of the U L<sub>III</sub> absorption edge of a 0.2 M solution of UO<sub>2</sub>Cl<sub>2</sub>, defined as 17 166 eV.

The data analysis was performed by the standard procedure<sup>9</sup> using the EXAFSPAK suite of programs developed by G. George of SSRL. The background was removed by fitting a polynomial to the preedge of the data such that the postedge spectrum followed the Victoreen function  $\mu_{vic}$ . The polynomial was subtracted from the data to give the spectrum  $\mu_{exp}$ . A spline function,  $\mu_{spline}$ , was chosen to minimize low-*R* peaks in the EXAFS Fourier transform. The EXAFS spectrum was obtained by the following function:  $\chi(k) = (\mu_{exp} - \mu_{spline}) / \mu_{vic}$ , where *k*, the electron energy in Å<sup>-1</sup>, is  $[(2m/h^2)(E - E_0)]^{1/2}$  and *E*<sub>0</sub> was defined as 17 180 eV.  $\Delta E_0$  was allowed to vary as a parameter during fitting of the EXAFS data; for a given fit,  $\Delta E_0$  was constrained to be identical for all scattering shells. For U(IV) complexes,  $\Delta E_0$  varied from -8.8 to -11.1 eV, and for U(III) complexes,  $\Delta E_0$  varied from -13.6 to -21.4 eV.

Fitting of the spectrum was done on the *k*<sup>3</sup> weighted data using the EXAFS equation

$$\chi(k) \cong S_0^2 \sum_{i=1}^n \frac{N_i S_i(k, R_i) F_i(k, R_i)}{k R_i^2} \exp\left(\frac{-2R_i}{\lambda(k, R_i)}\right) \times \exp(-2\sigma_i^2 k_i^2) \sin[2kR_i + \phi_i(k, R_i) + \phi_c(k)]$$

where *S*<sub>0</sub><sup>2</sup> is the scale factor, fixed at 0.9, *N*<sub>*i*</sub> the coordination number for shell *i*, was fixed at the value determined by crystallography, *S*<sub>*i*</sub> is the central atom loss factor for atom *i*, *F*<sub>*i*</sub> is the EXAFS scattering function for atom *i*, *R*<sub>*i*</sub> is the distance to atom *i* from the absorbing atom,  $\lambda_i$  is the photoelectron mean free path,  $\sigma_i$  is the Debye-Waller factor;  $\phi_i$  is the EXAFS phase function for atom *i*, and  $\phi_c$  is the EXAFS phase function for the absorbing atom. The program Feff<sup>6</sup> was used to calculate theoretical values for *S*<sub>*i*</sub>, *F*<sub>*i*</sub>,  $\lambda_i$ ,  $\phi_i$ , and  $\phi_c$  on the basis of atomic positions taken from the crystal structure of the most similar complex.

**Crystallography.** [Cp<sup>+</sup><sub>2</sub>UF]<sub>2</sub>. Dark blue-green crystals of the compound were grown by cooling a hexane solution to -20 °C. A suitable square prism measuring 0.27 × 0.27 × 0.14 mm was mounted on the end of a 0.2 mm diameter thin-walled glass capillary using Paratone N oil. The crystal was transferred to an Enraf-Nonius CAD-4 diffractometer and cooled to -111 °C under a cold stream previously calibrated by a thermocouple placed in the sample position. After centering, automatic peak search and indexing procedures indicated that the crystal had a primitive triclinic cell and yielded the unit cell parameters. The cell parameters and data collection parameters are given in Table 4.

The 8121 raw intensity data were converted to structure factor amplitudes and their esd's by correction for scan speed, background, and Lorentz-polarization effects.<sup>10</sup> Inspection of the intensity standards showed no decrease in intensity over the duration of data collection. Inspection of the azimuthal

(10) The data reduction formulas are

$$F_o^2 = \frac{\omega}{Lp} (C - 2B)$$

$$\sigma_o(F_o^2) = \frac{\omega}{Lp} (C + 4B)^{1/2}$$

$$F_o = (F_o^2)^{1/2}$$

$$\omega_o(F) = [F_o^2 + \sigma_o(F_o^2)]^{1/2} - F_o$$

where *C* is the total count of the scan, *B* is the sum of the two background counts,  $\omega$  is the scan speed used in deg/min, and

$$\frac{1}{Lp} = \frac{\sin 2\theta(1 + \cos^2 2\theta_m)}{1 + \cos^2 2\theta_m - \sin^2 2\theta}$$

is the correction for Lorentz and polarization effects for a reflection with scattering angle 2 $\theta$  and radiation monochromatized with a 50% perfect single-crystal monochromator with scattering angle 2 $\theta_m$ .

Table 4. Crystal Data

	[Cp <sup>+</sup> <sub>2</sub> UF] <sub>2</sub>	[Cp <sup>+</sup> <sub>2</sub> UO] <sub>2</sub>
space group	<i>P</i> $\bar{1}$	<i>P</i> $\bar{1}$
<i>a</i> , Å	11.363(4)	10.6985(8)
<i>b</i> , Å	14.963(3)	11.2046(8)
<i>c</i> , Å	17.845(4)	12.2575(9)
$\alpha$ , deg	89.81(2)	64.522(1)
$\beta$ , deg	76.86(2)	73.698(1)
$\gamma$ , deg	84.32(2)	89.862(1)
<i>V</i> , Å <sup>3</sup>	2939.7	1261.9(1)
<i>Z</i>	2	1
<i>d</i> (calcd) g/cm <sup>3</sup>	1.53	1.602
$\mu$ (calcd) cm <sup>-1</sup>	54.09	64.06
radiation ( $\lambda$ , Å)	Mo K $\alpha$ (0.710 73)	
monochromator	highly oriented graphite	
scan range, type	3° > 2 $\theta$ > 45°, $\theta$ -2 $\theta$	
scan speed, deg/min	3.4	
scan width, deg	$\Delta\theta = 0.60 + 0.35 \tan \theta$	
no. of rflns collected	8121; + <i>h</i> , ± <i>k</i> , ± <i>l</i>	5485
no. of unique rflns	7655	3906 ( <i>R</i> <sub>int</sub> = 0.071)
no. of rflns, <i>F</i> <sub>o</sub> <sup>2</sup> > 3 $\sigma$ ( <i>F</i> <sub>o</sub> <sup>2</sup> )	6339	2543 ( <i>I</i> > 3 $\sigma$ ( <i>I</i> ))
<i>R</i> , %	2.2	5.2
<i>R</i> <sub>w</sub> , %	2.4	7.3
<i>R</i> <sub>all</sub> , %	4.3	
GOF	1.12	3.12
largest $\Delta/\sigma$ in final least-squares cycle	0.05	0.0

scan data showed a variation of *I*<sub>min</sub>/*I*<sub>max</sub> = 0.85 for the averaged curve. An empirical absorption correction was applied to the intensity data on the basis of the average curve. Removal of redundant data (0, -*k*, -*l*) left 7655 unique data.

The uranium atom positions were obtained by solving the Patterson map. The solution indicated that the molecule was in space group *P* $\bar{1}$  with *Z* = 2 and that the asymmetric unit contained two crystallographically independent molecules, each having inversion symmetry. Refinement on the uranium positions followed by difference Fourier searches yielded the other heavy-atom positions. The heavy-atom structure was refined by standard least-squares and Fourier techniques. The heavy atoms were refined with isotropic and then anisotropic thermal parameters. The hydrogen positions were calculated on the basis of idealized bonding geometry and assigned thermal parameters equal to 1.15 Å<sup>2</sup> larger than the values for the carbon atom to which they were connected. The hydrogen positions were included in the structure factor calculations but not refined by least squares. Toward the end of the refinement, examination of the extinction test listing indicated that secondary extinction was occurring. The secondary extinction coefficient was initially set to 3.4 × 10<sup>-8</sup> and was refined. A final difference Fourier map showed no additional atoms in the asymmetric unit. No close (<3.5 Å) intermolecular contacts were found.

$$(11) \quad R = \frac{\sum (|F_o| - |F_c|)}{\sum |F_o|}$$

$$R_w = \left[ \frac{\sum (|F_o| - |F_c|)^2}{\sum w F_o^2} \right]^{1/2}$$

$$\text{GOF} = \left[ \frac{\sum (|F_o| - |F_c|)^2}{(n_o - n_v)} \right]^{1/2}$$

where *n*<sub>o</sub> is the number of observations, *n*<sub>v</sub> is the number of variable parameters, and the weights were given by

$$w = \frac{1}{\sigma^2(F_o)}$$

$$\sigma(F_o^2) = [\sigma_o^2(F_o^2) + (pF_o^2)^2]^{1/2}$$

where  $\sigma^2(F_o)$  is calculated as above from  $\sigma(F_o^2)$  and where *p* is the factor used to lower the weight of intense reflections.

The final residuals for 506 variables refined against the 6339 observed data with  $F_o > 3\sigma(F_o)$  were  $R = 2.23\%$ ,  $R_w = 2.58\%$ , and  $GOF = 1.12$ . The  $R$  value for all data (including unobserved reflections) was 4.34%. The quantity minimized by the least-squares refinements was  $w(|F_o| - |F_c|)^2$ , where  $w$  is the weight given to a particular reflection. The  $p$  factor, used to reduce the weight of intense reflections, was set to 0.03 initially and later changed to 0.02.<sup>11</sup> The analytical forms of the scattering factor tables for neutral atoms were used, and all non-hydrogen scattering factors were corrected for both the real and imaginary components of anomalous dispersion.<sup>12</sup> Inspection of the residuals ordered in the ranges of  $(\sin \theta)/\lambda$ ,  $|F_o|$ , parity, and values of the individual indexes showed no trends other than the previously mentioned secondary extinction. No reflections had anomalously high values of  $w\Delta^2$ . The largest positive and negative peaks in the final difference Fourier map have electron densities of 0.763 and  $-0.528 \text{ e } \text{\AA}^{-2}$ , respectively, and are associated with the uranium atom.

**[Cp<sup>+</sup><sub>2</sub>UO]<sub>2</sub>.** Brown crystals of the compound were grown by cooling a toluene solution from 100 °C to room temperature. A suitable block-shaped crystal measuring  $0.20 \times 0.16 \times 0.16 \text{ mm}$  was mounted on the end of a 0.2 mm thin-walled glass capillary using Paratone N oil. The crystal was transferred to a Siemens SMART diffractometer and cooled to  $-95 \text{ }^\circ\text{C}$  under a cold stream previously calibrated by a thermocouple placed in the sample position. After the crystal was centered, automatic peak search and indexing procedures indicated that the crystal had a primitive triclinic cell and yielded the unit cell parameters. The cell parameters and data collection parameters are given in Table 4. On the basis of a statistical analysis of intensity distribution and the successful solution and refinement of the crystal structure, the space group was found to be  $P\bar{1}$ .

An arbitrary hemisphere of data was collected using the default parameters for the diffractometer. The data were collected as 30 s images with an area detector. Two images were averaged to give the net image data. The image data were integrated to give intensity data using the program SAINT. The data provide 93% coverage at 0.86 Å resolution and 85% at 0.83 Å. The 5485 raw intensity data were converted to structure factor amplitudes and their esd's by correction for scan speed, background, and Lorentz-polarization effects.<sup>10</sup> Inspection of the intensity standards showed no decrease in intensity over the duration of data collection. An empirical absorption correction using an ellipsoidal model for the crystal was applied to the intensity data on the basis of the intensities of all intense equivalent reflections ( $T_{\text{max}} = 0.823$ ,  $T_{\text{min}} = 0.621$ ). Averaging equivalent reflections gave 3906 unique data ( $R_{\text{int}} = 0.071$ ).

(12) Cromer, D. T.; Waber, J. T. In *International Tables for X-ray Crystallography*; Kynoch Press: Birmingham, England, 1974; Vol. IV.

The uranium atom positions were obtained by direct methods. Refinement on the uranium positions followed by difference Fourier searches yielded the other heavy-atom positions. The heavy-atom structure was refined by standard least-squares and Fourier techniques. The heavy atoms were refined with anisotropic thermal parameters, except for C24-C29, which form a disordered *tert*-butyl group. The disorder was modeled using two sets of methyl carbon atoms rotated by ca. 60° with respect to each other. The occupancy of the disordered carbon atoms was allowed to vary but remained near 0.5. The hydrogen positions, based upon idealized bonding geometry, were included in the structure factor calculations but not refined by least squares. Toward the end of the refinement, examination of the extinction test listing indicated that secondary extinction was occurring. The secondary extinction coefficient was refined to  $1.05 \times 10^{-6}$ . A final difference Fourier map showed no additional atoms in the asymmetric unit. No close ( $<3.5 \text{ \AA}$ ) intermolecular contacts were found.

The final residuals for 252 variables refined against the 2543 unique data with  $I > 3\sigma(I)$  were  $R = 5.2\%$ ,  $R_w = 7.3\%$ , and  $GOF = 3.12$ . The quantity minimized by the least-squares refinements was  $w(|F_o| - |F_c|)^2$ , where  $w$  is the weight given to a particular reflection. The  $p$  factor, used to reduce the weight of intense reflections, was set to 0.03.<sup>11</sup> The analytical forms of the scattering factor tables for neutral atoms were used, and all non-hydrogen scattering factors were corrected for both the real and imaginary components of anomalous dispersion.<sup>12</sup>

Inspection of the residuals ordered in the ranges of  $(\sin \theta)/\lambda$ ,  $|F_o|$ , parity, and values of the individual indexes showed no trends other than the previously mentioned secondary extinction. No reflections had anomalously high values of  $w\Delta^2$ . The largest positive and negative peaks in the final difference Fourier map have electron densities of 1.81 and  $-2.15 \text{ e } \text{\AA}^{-2}$ , respectively.

**Acknowledgment.** We thank Dr. Fred Hollander for helpful discussions about the crystal structure determinations. W.W.L. thanks the National Science Foundation for a graduate fellowship. This work was partially supported by the Director, Office of Energy Research, Office of Basic Energy Sciences, Chemical Sciences Division, of the U.S. Department of Energy under Contract No. DE-AC03-76SF00098.

**Supporting Information Available:** Tables of atomic positions and anisotropic thermal parameters for  $[\text{Cp}'_2\text{UF}]_2$  and  $[\text{Cp}^+_2\text{UO}]_2$ . This material is available free of charge via the Internet at <http://pubs.acs.org>.

OM980600V